Studies on Age-related Hearing Loss in Mouse Cochlea using DNA Microarrays

（ＤＮＡマイクロアレイを用いたマウス蝸牛の加齢性難聴に関する研究）

A Dissertation

Presented to the Faculty of the Graduate School of Agricultural and Life Sciences, University of Tokyo

for the Degree of Doctor of Philosophy

by

Shinichi Someya

染　谷　慎　一

January, 2005

Abstract

Studies on Age-related Hearing Loss in Mouse Cochlea using DNA Microarrays

Shinichi Someya

University of Tokyo

2005

Age-related hearing loss (AHL) is the loss of hearing that gradually occur in most individuals as they grow older (Berlin, 2000; Erway *et al.*, 1996). AHL may be caused by accumulated exposure to noise, environmental chemical exposure, diet, and genetics (Gacek and Schuknecht, 1969; NIDCD, 2004). However, the molecular mechanisms of AHL remain unknown. In order to understand the molecular mechanisms of AHL, I examined gene expression profiles of AHL in cochlea of DBA/2J (DBA) mice, a well-known model of AHL, and then tested whether mitochondrial DNA (mtDNA) mutations, known to be associated with the aging process, play a causal role in the progression of AHL using $Polg^{D257A}$ (D257A) knock-in mice, which exhibit increased spontaneous mutation rates in mtDNA during aging. In order to understand how AHL can be retarded, I examined effects of calorie restriction (CR) on the progression of AHL using C57BL/6 (B6) mice.

The DBA strain exhibits early onset of hearing loss and has been extensively studied as a model of AHL (Zheng *et al.*, 1999; Johnson *et al.*, 1997). The auditory brainstem response (ABR) results revealed that aged DBA mice (36 weeks of age, n = 5) exhibited severe hearing loss, whereas control DBA mice (7 weeks of age, n = 5) exhibited moderate hearing loss. Histological analysis revealed that aged DBA mice exhibited severe loss of hair cells and spiral ganglion cells, whereas control DBA mice exhibited mild degeneration of the organ of Corti. Aged DBA cochlea (n = 3) and control DBA cochlea (n = 3) were compared using microarrays representing 22,626 genes and ESTs. The gene expression profile results revealed suppression of hearing-related genes, decreased energy metabolism, and induction of apoptosis-related genes, such as *Bak1* and *Scotin*, which mediate p53-dpendent apoptosis (Berlin, 2000; Johnson *et al.*, 1997; Jimenez *et al.*, 2001; Keithley *et al.*, 2003; Bourdon *et al.*, 2002). AHL was also characterized by gene expression profiles consistent with suppression of neurotransmission, ion transport, muscle contraction, structural modulation, DNA synthesis, DNA repair, protein synthesis, and induction of stress response, inflammatory response, and proteolysis. Taken together, these results suggest that AHL develops by mechanisms that may be related to decreased energy metabolism and induction of apoptosis.

The D257A mouse was created by introducing a specific point mutation in the exonuclease domain of DNA polymerase gamma (*Polg*). Because this mouse model expresses a mtDNA polymerase with decreased proof-reading activity, D257A mice exhibit increased spontaneous mutation

rates in mtDNA, which in turn accelerate several aspects of aging (Kujoth e*l al.*, 2005). The ABR results revealed that old D257A mice (9 months of age, n = 5) exhibited moderate hearing loss, whereas young D257A mice (2 months of age, n = 5), young wild-type (wt) mice (2 months of age, n =5), and old wt mice (9 months of age, n =5) exhibited normal hearing. Histological analysis revealed that old D257A mice exhibited server loss of spiral ganglion cells and mild loss of hair cells, whereas old wt mice and young D257A mice exhibited no degeneration of the organ of Corti. Old D257A cochlea (n =5) and old wt cochlea (n = 5) were compared using microarrays representing 45,037 genes and ESTs. The gene expression profile results revealed suppression of hearing-related genes, decreased energy metabolism, and induction of apoptosis-related genes, such as *Check1*, *Bcl2l11*, and *Tnfrsf1a*, which mediate p53-dependent apoptosis (Vogelstein *et al.*, 2000; Prives and Hall, 1999; Urist *et a*l., 2004; Gross *et al.*, 1999; O'Connor *et al.*, 1998; Bigelow *et al.*, 2004; Inagaki-Ohara *et al.*, 2001). The TUNEL (Terminal deoxynucleotidyl transferase biotin-dUTP nick end labeling) assay results revealed that TUNEL-positive cells were found in spiral ganglion cells in the young D257A mice, but not in the young wt mice. Taken together, these results suggest that mtDNA mutations play a causal role in the progression of AHL, and that apoptosis plays a role in the progression of AHL. Mitochondrial DNA damage can activate p53, which in turn induces apoptosis (Vogelstein *et al.*, 2000; Prives and Hall, 1999; Urist *et a*l.,). Thus, these results from the DBA mouse and D257A mouse studies suggest that

AHL develops by mechanisms that may be related to induction of apoptosis and mitochondrial dysfunction.

CR, the only intervention known to retard aging in mammals, results in delayed onset of age-associated pathological and physiological changes, and extends lifespan in mammals (Lee *et al.*, 2002; Lee *et al.*, 1999; Lee *et al.*, 1999; Prolla, 2002). The ABR results revealed that CR B6 mice (15 months of age, 63 kcal/week of restricted diet, n = 6) retained good hearing, whereas control B6 mice (15 months of age, 84 kcal/week of control diet, n = 6) exhibited moderate hearing loss. Histological analysis revealed that CR B6 mice exhibited no degeneration of the organ of Corti, whereas control B6 mice exhibited severe loss of hair cells and spiral ganglion cells. CR B6 cochlea (n = 3) and control B6 cochlea (n = 3) were compared using microarrays representing 45,037 genes and ESTs. The gene expression profile results revealed that AHL-related changes in the gene expression were remarkably reversed by CR. CR resulted in induction of hearing-related genes, energy metabolism-related genes such as *Sirt1*, which mediates life-extending effects of CR (Lin *et al.*, 2002; Vaziri *et al.*, 2001; Tissenbaum *et al.*, 2001; Gasser *et al.*, 2001; Lin *et al.*, 2000), and suppression of apoptosis-related genes such as *Mdm2* and *Il6*, which mediate p53-dependent apoptosis (Prives and Hall, 1999; Vogelstein *et al.*, 2000; Afford *et al.*, 1992; Margulies and Sehgal, 1993). Taken together, these results suggest that CR prevents the progression of AHL by induction of increased energy metabolism and suppression of apoptosis. CR extends lifespan in numerous species (Lee *et al.*, 2002; Lee *et al.*, 1999; Lee *et al.*,

1999; Prolla, 2002; Drew *et al.*, 2002). In yeast, the *SIR2* gene mediates the life-extending effects of CR (Lin *et al.*, 2002; Vaziri *et al.*, 2001; Tissenbaum *et al.*, 2001; Gasser *et al.*, 2001; Lin *et al.*, 2000). The mammalian *SIR2* orthologue, *Sirt1* also mediates cell survival in mammals, and Sirt1 protein represses p53-dependent apoptosis in response to DNA damage in mammals (Koubova *et al.*, 2003; Luo *et al.*, 2001; Picard *et al.*, 2004). Thus, these suggest that CR retards the progression of AHL by mechanisms that may be related to induction of energy metabolism-related genes such as *Sirt1*, and suppression of p53-dependent apoptosis.

Based on these findings, I propose a model of how CR retards the progression of AHL: CR causes a metabolic shift toward increased energy metabolism, perhaps by increasing the NAD^+/NADH ratio. This metabolic shift induces energy metabolism-related genes such as *Sirt1*, which in turn represses p53-dependent apoptosis by interacting with p53. This repression leads to preventing the cochlea from loss of hair cells and spiral ganglion cells, and hence to slowing down the progression of AHL. I also propose a model of how AHL develops in mammals: mtDNA mutations and other lesions accumulate in DNA in the cochlea during aging, and the resulting DNA damages result in the induction of apoptosis-related genes such as *Chek1, Bak, Scotin*, which in turn induce p53-dependent apoptosis by interacting with p53. This leads to loss of hair cells and spiral ganglion cells in the cochlea. AHL develops when loss of these cells reaches a critical level.

CR extends lifespan in yeast, and this effect requires Sir2 protein (Lin *et al.*, 2002; Vaziri *et al.*, 2001; Tissenbaum *et al.*, 2001; Gasser *et al.*, 2001; Lin *et al.*, 2000; Brunet *et al.*, 2004). Resveratrol, a polyphenol found in red wine, mimics CR by activating Sir2, and extends lifespan in yeast (Howltz *et al.*, 2003; Wood *et al.*, 2004). Thus, polyphenols which activate Sirt1 in mammals could be good candidates for a new preventive intervention or new functional supplement which could slow down the progression of AHL in humans. Our laboratory has identified several candidate polyphenols from Japanese persimmons and Chinese white teas (Suzuki *et al.*, 2005; Hu *et al.*, 2005). Currently, we are planning to test effects of these polyphenols on the progression of AHL.

Acknowledgements

Completing the work described in this thesis dissertation was a project that involved many individuals. I am deeply indebted to my thesis advisor, Dr. Masaru Tanokura. Dr. Tanokura provided patient and constant guidance throughout this work, and also kept my motivation high. I am also deeply indebted to my thesis advisor and collaborator, Dr. Tomas A. Prolla, who made a significant contribution to this work. Without his help and constant guidance, the final stages of this work would have progressed at a much slower pace. I am also very grateful to my thesis advisor, Dr. Yamasoba, who has worked in close collaboration with me in the ABR analysis, dissection of cochlea from mice, and histopathology.

Since our laboratory had little experience with DNA microarrays, I learned many techniques, such as isolation of total RNA from mouse cochlea, gene expression analysis, and data analysis, in the laboratory of Dr. Tomas A. Prolla at University of Wisconsin-Madison. I also wish to thank my thesis committee members, Dr. Keiko Abe, Dr. Makoto Shimizu, and Dr. Nagato Miyawaki for their helpful guidance.

Finally, I wish to thank my wife Satoko for her patience and support, which were essential for the rapid progress of this work.

Table of Contents

List of Figures

List of Tables

Chapter 1: Introduction

Age-related hearing loss (AHL) is characterized by the progressive deterioration of auditory sensitivity associated with aging (Berlin, 2000; Johnson *et al.*, 1997; Jimenez *et al.*, 2001; Keithley *et al.*, 2003). Histological changes associated with aging occur throughout the auditory system from the hair cells of the cochlea to the auditory cortex in the brain (Figure 1-1) (John *et al.*, 1989; Johnson and Zheng, 2001; Kros *et al.*, 1998; McFdden *et al.*, 1998; Schwartz *et al.*, 2002; Seidman, 2002; Seideman *et al.*, 2000; Takahashi *et al.*, 1999). Gacek and Schuknecht identified 4 sites of aging in the cochlea and divided AHL into four types based on these sites (Gacek and Schuknecht, 1969): 1) Sensory AHL results from epithelial atrophy with loss of sensory hair cells and supporting cells in the organ of Corti, which originates in the basal turn of the cochlea of the inner ear and slowly progresses toward the apex. 2) Neural AHL results from atrophy of nerve cells in the cochlea and central neural pathways. Effects are not noticeable until old age because pure-tone average is not affected until 90% of neurons are lost (Jimenez *et al.*, 2001; Berlin, 2000). 3) Metabolic AHL results from atrophy of the stria vascularis. The stria vascularis usually maintains the chemical and bioelectric balance and metabolic health of the cochlea (Willems, 2004; Willott, 2001; Yost, 2000). 4) Mechanical AHL results from thickening and secondary stiffening of the basilar membrane of the cochlea (Wilott *et al.*, 1998). The thickening is more severe in the basal turn of the

Figure 1-1. The cochlea and the organ of Corti. (a) A three-dimensional section of the cochlea, showing the compartments, tectorial membrane, and the organ of Corti. (b) Diagrammatic and sectional views of the receptor hair cells and spiral ganglion cells of cochlea nerve in the organ of Corti (Martini, 2004).

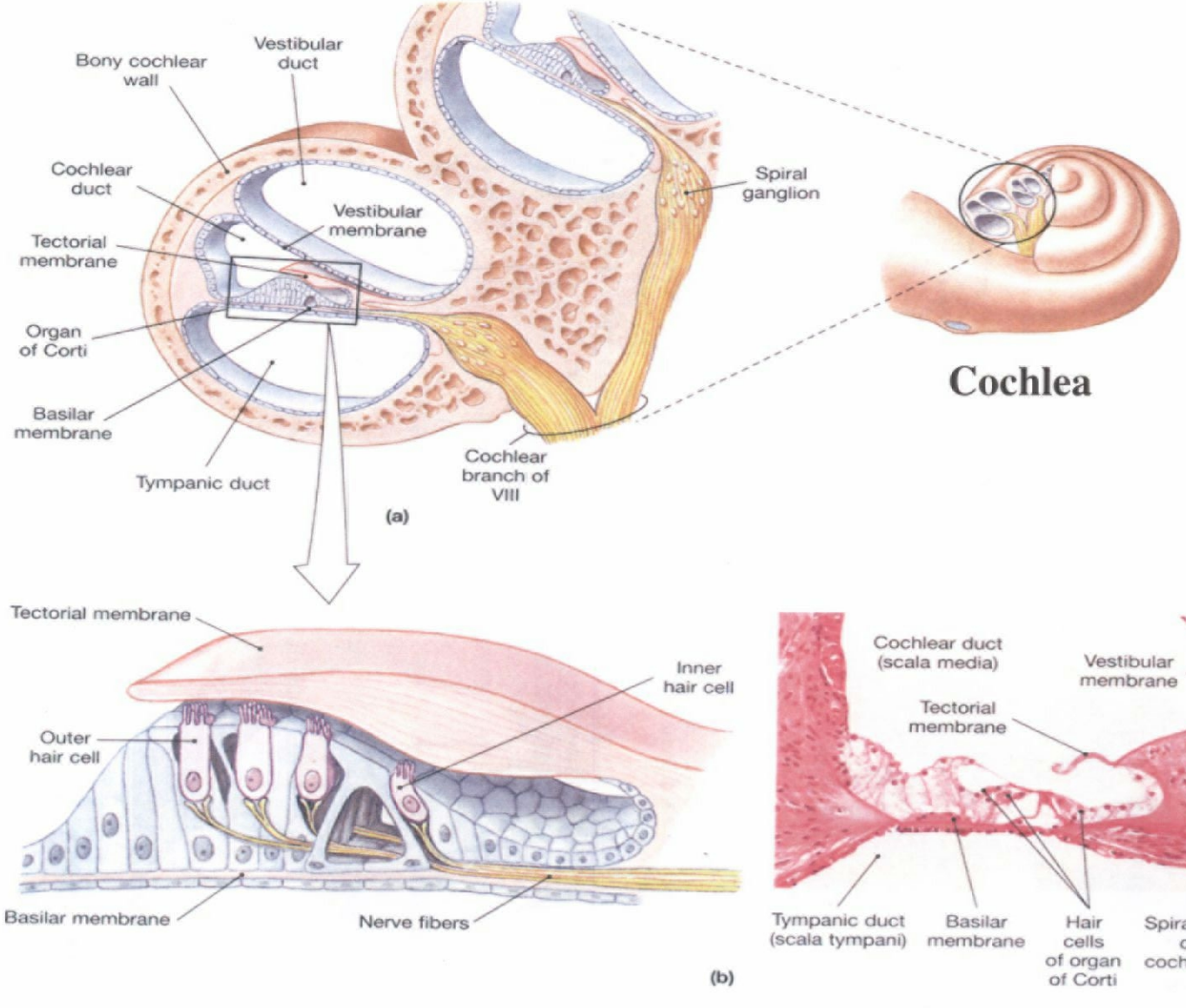
Bony cochlear wall
Vestibular duct
Cochlear duct
Vestibular membrane
Tectorial membrane
Organ of Corti
Basilar membrane
Tympanic duct
Cochlear branch of VIII
Spiral ganglion
(a)
Cochlea
Tectorial membrane
Inner hair cell
Outer hair cell
Basilar membrane
Nerve fibers
Cochlear duct (scala media)
Vestibular membrane
Tectorial membrane
Tympanic duct (scala tympani)
Basilar membrane
Hair cells of organ of Corti
Spiral ganglion cells of cochlear nerve
(b)

cochlea where the basilar membrane is narrow (Johnson *et al.*, 1997; Johnson *et al.*, 2000). This correlates with a gradually sloping high-frequency sensorineural hearing loss that is slowly progressive (Berlin, 2000; Johnson *et al.*, 1997; Johnson *et al.*, 2000). The development of AHL typically involves simultaneous changes at multiple sites (Gacek and Schuknecht, 1969).

AHL is an important problem in society. In the US, it is estimated that approximately 30-35 percent of people between 65 and 75 years of age, and 40-50 percent of people over 75 years of age, have a hearing loss (NIDCD, 2004; Seidman, 2002). This older population (people over 65 years of age) numbered 35.9 million in 2003, representing 12.3% of the U.S. population (Administration on aging, 2004). By 2030, this population will increase by more than twice their number (Administration on aging, 2004). On a comparative basis, people over 65 years of age represented 12.4% of the population in the year 2000, but are expected to grow to be 20% of the population by 2030 (Administration on aging, 2004). Nonetheless, no preventive or therapeutic interventions have been established for AHL (NIDCD, 2004; Seidman, 2002; Seidman, 2000; Seidman *et al.*, 2000; Seidman *et al.*, 2002).

Mitochondrial mutations may contribute to AHL (Damdimpopoulos *et al.*, 2002; Fischel-Ghodsian, 1999; Johnson *et al.*, 2001). Many mitochondrial disorders appear late in life (Drew and Leeuwenburgh, 2004; Green and Leeuwenburgh, 2002; Kanungo, 1994; Patenaude *et al.*, 129), and

tend to affect cell types that are postmitotic, and have high energy requirements, including those that are heavily involved in ion pumping (Fischel-Ghodsian, 1999; Mekerhofer *et al.*, 2004; Pollack and Leeuwenburgh, 2001; Pollack *et al.*, 2002). Mitochondria defects commonly appear in the brain, eye, and ear (Scheffler, 1999). Since mitochondrial DNA (mtDNA) is situated near the major site of reactive oxygen species (ROS) production, it becomes particularly vulnerable to ROS damage (Dirks and Leeuwenburgh, 2002; Harmon, 1956; Fischel-Ghodsian, 1999; Hosokawa, 2002). In addition, mtDNA is not protected by histones and has more limited repair mechanisms than does nuclear DNA (Fischel-Ghodsian, 1999). While some repair and maintenance mechanisms exist for mtDNA, they are in general limited compared with those for nuclear DNA. Mitochondrial DNA polymerase gamma (*Polg*) has proofreading capability that corrects DNA replication errors resulting from nucleotide misincorporation (Kujoth e*l al.*, 2005; Tissenbaum *et al.*, 2004). In *S. cerevisiae*, a specific point mutation in the exonuclease domain of the *Polg* resulted in decreased proofreading activity, which in turn led to a 200-hold increase in mtDNA mutation rates (Kujoth e*t al.*, 2005; Tissenbaum *et al.*, 2004). In fact, inherited point mutations can lead to mitochondrial syndromes that can have deafness, such as MELAS (mitochondrial encephalomyopathy, lactic acidosis and stroke-like episodes), MERRF (myoclonic epilepsy and ragged red fibres), and MEADF (myoclonic epilepsy, ataxia and deafness) (Fischel-Ghodsian, 1999).

The mouse is an excellent animal model for the study of human genetic deafness (Zheng *et al.*, 1999). The mouse cochlea is anatomically

similar to that of humans, and hereditary abnormalities of the inner ear have been shown to be similar in both humans and mice (Erway *et al.*, 1996; Fischel-Ghodsian; Johnson *et al.*, 1997; Weil *et al.*, 1997; Weil *et al.*, 1996). Because of the similarities between the human and the mouse auditory systems, identification of the genes causing hearing impairment or deafness in mice may also allow for the identification of homologous human genes and genetic diseases (Erway *et al.*, 1996; Fischel-Ghodsian; Johnson *et al.*, 1997; Zheng *et al.*, 1999). In fact, genetic analysis of mouse deafness mutations already has proven valuable for the identification of genes causing human nonsyndromic deafness, such as *MYO7A, MYO15*, and *POU4F3* (Johnson *et al.*, 1997; Erway *et al.*, 1996; Di Palma *et al.*, 2001; Hudspeth *et al.*, 1998; Noben-Trauth *et al.*, 2003; Robertoson *et al*, 1998; Skvorak *et al.*, 1999, Siemens *et al*, 2004; Sollner *et al.*, 2004; Wada *et al.*, 2001). In contrast, certain inbred strains of mice exhibit a progressive, nonsyndromic hearing loss, with onset at more advanced ages (Zheng *et al.*, 1999). These strains, such as DBA/2J and C57BL/6, have provided useful models for human AHL (Zheng *et al.*, 1999; Johnson *et al.*, 1997; Johnson *et al.*, 2000; Zheng *et al.*, 2001).

AHL may be caused by multifactor, such as arteriosclerosis, diet, accumulated exposure to noise, drug, environmental chemical exposure, stress, and genetics (Gacek and Schuknecht, 1969; NIDCD, 2004). mtDNA mutations may also contribute to AHL (Damdimpopoulos *et al.*, 2002; Fischel-Ghodsian, 1999; Johnson *et al.*, 2001). However, the molecular mechanisms of how AHL develops remain unknown. Thus, in order to

understand the molecular mechanisms of AHL, I first examined gene expression profiles of AHL in cochlea of DBA/2J (DBA) mice, a well-known model of AHL, and then tested whether mitochondrial DNA (mtDNA) mutations, known to be associated with the aging process, play a causal role in the progression of AHL using $Polg^{D257A}$ (D257A) mice. In order to understand how AHL can be retarded, I examined effects of calorie restriction (CR) on the progression of AHL using C57BL/6 (B6) mice.

Chapter 2: Materials and Methods

DBA/2J mice

Male DBA/2J (DBA) mice, 4-5 weeks of age, were purchased from Clear Japan, Inc. (Tokyo, Japan). The mice were divided into two groups: a 7-week-old control group (control), and a 37-week-old group (aged). All mice were housed in the standard animal facility under normal mouse rearing conditions at Department of Otolaryngology, University of Tokyo.

$Polg^{D257A}$ mice

Male $Polg^{D257A}$ (D257A) transgenic mice were created and housed in the specific pathogen-free facility at Departments of Genetics and Medical Genetics, University of Wisconsin-Madison. The mice were divided into four groups: a 2-month-old wild-type group (young wt), a 2-month-old mutant group (young D257A), a 9-month-old wild-type group (old wt), and a 9-month-old mutant group (old D257A). All mice were housed individually and provided acidified water ad libitum in the specific pathogen-free facility at the University of Wisconsin-Madison.

C57BL/6 mice

Male C57BL/6 (B6) mice, 1.5 months of age, were purchased from Charles River Laboratories (Wilmington, MA). The mice were housed singly in the specific pathogen-free facility at University of Wisconsin-Madison, and

provided a nonpurified diet and acidified water ad libitum. The mice were then divided into two groups: a 15-month-old control group (control) and a 15-month-old calorie-restricted group (CR). Each control B6 mouse was fed 84 kcal/week of the control diet (TD91349; Teklad, Madison, WI), which is 5-20% less than the range of individual ad libitum intakes. This dietary intake was used so that the control B6 mice were not obese. Each CR B6 mouse was fed 62 kcal/week of the restricted diet (TD91351; Teklad), resulting in a 26% reduction of calorie intake. The latter diet was enriched in protein, vitamin, and minerals such that CR and control mice were fed nearly identical amounts of these components (Pugh et al., 1999; Weindruch *et al.*, 2002).

Assessment of hearing

When mice reached the designated age, auditory brainstem responses (ABRs) were measured with a tone burst stimulus (4, 8, and 16 kHz) in the mice using an ABR recording system (Intelligent Hearing System, Miami, FL) (Figure 2-1). Animals were anesthetized with a mixture of xylazine hydrochloride (10 mg/kg, i.m.) and ketamine hydrochloride (40 mg/kg, i.m.), and needle electrodes were placed subcutaneously at the vertex (active electrode), beneath the pinna of the measured ear (reference electrode), and beneath the opposite ear (ground). The stimulus duration, presentation rate, and rise/fall time were 5 ms, 19.3/s, and 1 ms respectively. Responses of 1024 sweeps were averaged at each intensity level (5 dB steps) to assess threshold. One hundred dB was defined as the maximum sound

Figure 2-1. Auditory brainstem response analysis. The auditory brainstem response analysis (ABR) is an electrical response starting in the inner ear that travels through the auditory pathway to the auditory cortex. The electrodes are placed at the vertex (across the top) of the animal's scalp and on each earlobe. Earphones are placed over the ears to deliver a series of tone noises to each ear separately. The electrodes measure the responses to the tone sound from the stimulus to the ear, the hearing nerve, the balance nerve and the brain stem.

ABR Sound Detection System

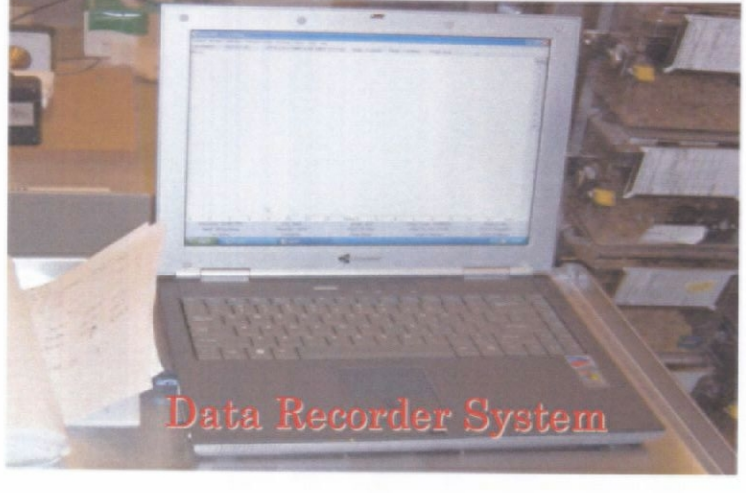

Detection of Sound

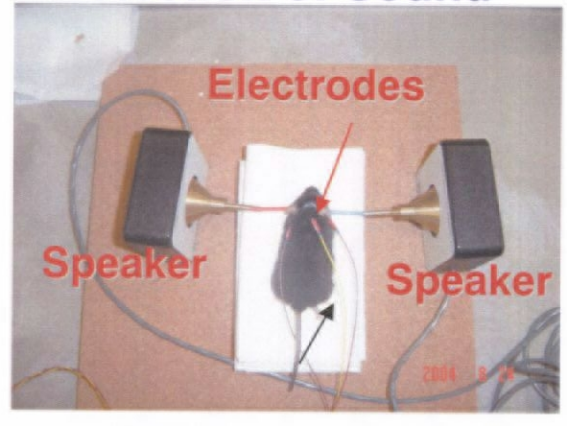

ABR Patterns

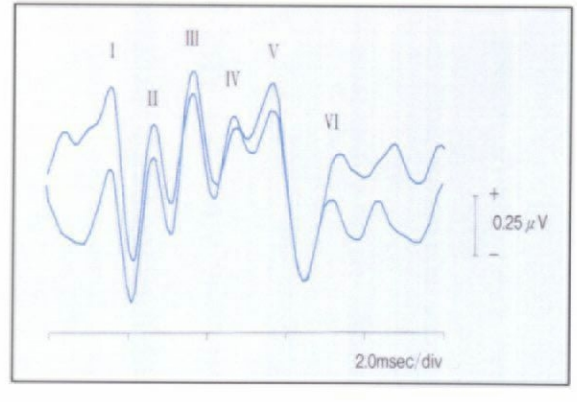

pressure. Threshold was defined as the lowest intensity level at which a clear reproducible waveform was visible in the trace. We used five mice per group for the DBA mouse study and the D257A mouse study, and six mice per group for the B6 mouse study.

Histolopathology

Mice were decapitated under deep anesthesia with a mixture of xylazine hydrochloride and ketamine hydrochloride. After removing the temporal bones, the cochleae were perfused with 2 % paraformaldehyde and 2.5% glutaraldehyde in phosphate buffered saline (PBS) through the round and oval windows, immersed in the same fixative for 24 h, and decalcified in 10% EDTA (pH 7.2) for 24 h. The cochleae were then rinsed with PBS, dehydrated through a graded series of alcohol, and embedded in epoxy resin. Thin sections cut parallel to the modiolus were stained with 0.5% toluidine blue and were observed under a light microscope. We used two mice per group for all the studies.

Sample preparations and hybridization for gene expression profiling

Five days after the ABR measurements, the mice were killed by cervical dislocation, and the cochleae were dissected, placed in a microcentrifuge tube, flash-frozen in liquid nitrogen, and stored at -80℃. Total RNA was extracted from cochlea tissue by using TRIZOL reagent (Life Technologies, Inc., Grand Island, NY). Detailed protocols for hybridization for gene expression analysis using Affymetrix microarrays have been

described by Prolla, Lee *et al.*, Edwards *et al.*, and Affymetrix (Prolla, 2002; Lee *et al.*, 2004; Edwards *et al.*, 2003; Affymetirx, 2004). Ten micrograms of total RNA were converted into double-stranded cDNA (ds-cDNA) by using SuperScript Choice System (Life Technologies, Inc., Grand Island, NY) with an oligo-dT primer containing a T7 RNA polymerase promoter (Genset, La Jolla, CA)(Figure 2-2). After second-stranded synthesis, the reaction mixture was extracted with phenol-chloroform-isoamyl alcohol, and ds-DNA was recovered by ethanol precipitation using Pellet Paint Coprecipitant (Novagen, Madison, WI). Biotin-labeled antisense cRNA was synthesized in vitro using a high-yield RNA transcript labeling kit (BioArray, Enzo, Farmingdale, NY). The biotin-labeled antisense cRNA was purified using the RNeasy affinity column (Qiagen) and fragmented randomly to sizes ranging from 35 to 200 bases by incubating at 94℃ for 35 min. The hybridization cocktail (200 μl) containing 10 μl of fragmented cRNA was injected into the MOE 430A arrays for the DBA mouse study and the Mouse Genome 430 2.0 arrays for the D257A mouse study and the B6 mouse study (Affymetirx, Santa Clara, CA). The GeneChip was placed in a 45℃ oven at 60 rpm for 16 h. After hybridization, the GeneChips were washed and stained in a fluidic station (Affymetrix GeneChip Fluidics Station 400) with signal amplification protocol using antibody. The MOE 430A GeneChips were scanned at a resolution of 6 μm twice using a Hewlett Packard GeneArray Scanner, and the Mouse Genome 430 2.0 GeneChips were scanned at a resolution of 2.5 μm once using GeneChip Scanner 3000.

Figure 2-2. The schematic outline of the gene expression analysis. Double stranded-cDNA is synthesized from total RNA samples, isolated from cochlea tissue. An *in vitro* transcription (IVT) reaction is then done to produce biotin-labeled cRNA from the cDNA. The cRNA is fragmented before hybridization. The cRNA sample is then hybridized to the probe array during a 16-hour incubation. Immediately following the hybridization, the probe array undergoes an atutomated washing and staining protocol on the fluidics station. Once the probe array has been hybridized, washed, and stained, it is scanned. The software defines the probe cells and computes an intensity for each cell. Data is analyzed using the Microarray Suit Expression Analysis software (Affymetirx, 2004).

Target Preparation

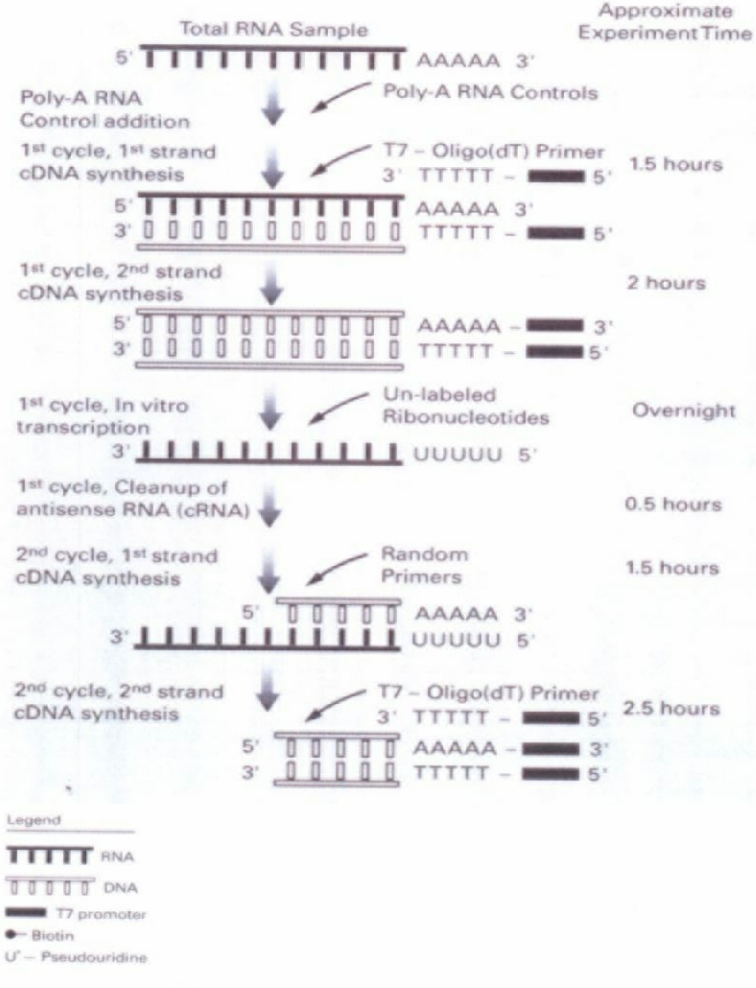

Target Hybridization, Probe Wash and Staining, Probe Array Scan

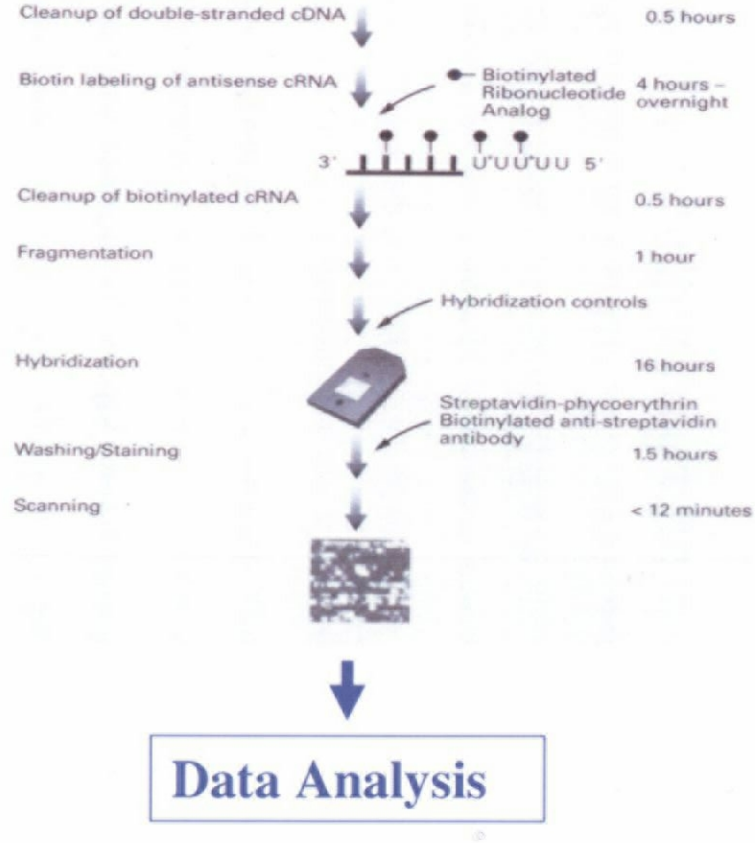

Data analysis

Detailed protocols for data analysis of Affymetrix microarrays and extensive documentation of the sensitivity and quantitative aspects of the methods have been described by Prolla, Edwards *et al.*, Bowtell and Sambrook, Speed, Stekel, and Liphshutz *et al.* (Prolla, 2002; Edwards *et al.*, 2003; Edwards *et al.*, 2004; Bowtell and Sambrook, 2002; Speed, 2003; Stekel, 2003; Liphshutz *et al.*, 1999): The Affymetrix Genechip was built on the basis of the cDNA sequences from the UniGene and TIGR databases. The MOE 430A array allows measurement of mRNA levels for 22,626 genes and ESTs. The Mouse Genome 430 2.0 array allows measurement of mRNA levels for 45,037 genes and ESTs. Approximately 20 probe pairs of oligonucleotide probes in a probe set (total of 40 probes; 20 for perfect match and 20 for mismatch control probes) are used to measure the transcript level of a gene. Each probe pair consists of a perfect match (PM) probe and a mismatch probe (MM), which allow direct subtraction of cross-hybridization signals after background subtraction. Affymetrix software determines the presence of mRNA in the samples and computes the signals of probe sets. The software calculates differences and ratios between perfect match and mismatch signals, which are representative of the hybridization levels of their targets in each probe set. These values are integrated to make a matrix-based decision concerning the presence or absence of an mRNA molecule in a sample. To determine relative mRNA levels, the average of the differences representing PM minus MM for each gene-specific probe family is calculated after removing the maximum, the minimum, and any outliers

beyond 3 standard deviations. Signals in each image are normalized to minimize an overall variability in hybridization intensities by a global scaling method. Global scaling is the computational technique in which the average signal of all probe sets in an image is scaled to target average intensity by multiplying a scaling factor. This scaling factor, 1500, was multiplied to each probe set signal to give the raw signal intensity. All genes considered absent as determined by Affymetrix software for all groups were eliminated from our analysis. Genes that had a small *P* value (less than 0.01), had a large fold change (more than 1.1), and had at least one present call were categorized as genes significantly altered in the expression by AHL. To determine the effects of AHL for the DBA mouse study, each control DBA mouse (n = 3) was compared to each aged DBA mouse, generating a total of nine pairwise comparisons. To determine the effects of AHL for the D257A mouse study, each old wt mouse (n = 5) was compared to each old D257A mouse (n = 5), generating a total of twenty-five pairwise comparisons. To determine the effects of CR for the B6 mouse study, each control sample (n = 3, two mice per GeneChip) was compared to each CR sample (n = 3, two mice per Genechip), generating a total of nine pairwise comparisons.

TUNEL assay

POD In Situ Cell Death Detection Kit (Beringer Mannheim Inc., Berlin, German) was used to detect TUNEL (terminal deoxynucleotidyl transferase (TdT)-mediated deoxyuridine triphosphate (dUTP)-biotin nick end labeling)-positive cells. One slide from each mouse was deparafinized

and rehydrated. To block endogenous peroxidase activity, the specimens were treated with 0.3% hydrogen peroxidase in ethanol for 30 min at room temperature. After washing with PBS, the specimens were incubated with 0.1% Triton X in 0.1% sodium citrate for 2 min on ice to permiabilize the cells, and were incubated with TdT and a nucleotide mixture for 60 min at 37℃ in a humidified chamber. After washing three times with PBS, a POD-conjugated antifluoresenin antibody was applied for 30 min at 37℃ in a humidified chamber, and the nick end labeling was visualized with diaminobenzdine (DAB) solution.

Chapter 3: Gene Expression Profile of Age-related Hearing Loss in Cochlea of DBA/2J Mice

Introduction

The DBA/2J strain exhibits early onset of hearing loss and has been extensively studied as a model of AHL (Zheng *et al.*, 1999; Johnson *et a*l., 2000). The mouse cochlea is anatomically similar to that of humans, and hereditary abnormalities of the inner ear have been shown to be similar in both humans and mice (Erway *et al.*, 1996; Fischel-Ghodsian; Johnson *et al.*, 1997). Because of the similarities between the human and the mouse auditory systems, identification of the genes causing hearing impairment or deafness in mice may also allow for the identification of homologous human genes and genetic diseases (Erway *et al.*, 1996; Fischel-Ghodsian; Johnson *et al.*, 1997; Zheng *et al.*, 1999). In fact, genetic analysis of mouse deafness mutations already has proven valuable for the identification of genes causing human nonsyndromic deafness, such as *MYO7A, MYO15*, and *POU4F3* (Johnson *et al.*, 1997; Erway *et al.*, 1996). In contrast, certain inbred strains of mice exhibit a progressive, nonsyndromic hearing loss, with onset at more advanced ages (Zheng *et al.*, 1999). These strains, such as DBA/2J, have provided useful models for human AHL (Zheng *et al.*, 1999; Johnson *et al.*, 1997). In order to understand the molecular mechanisms of AHL, I first examined gene expression profiles of AHL in cochlea of the DBA mice.

ABR analysis

To assess hearing impairment, ABR thresholds were measured at 4 kHz, 8 kHz, and 16 kHz. The mean of ABR thresholds for the control DBA mice were determined to be 56.0 dB SPL at 4 kHz, 54.9 dB SPL at 8 kHz, and 65.9 dB SPL at 16 kHz, exhibiting moderate hearing loss (Figure 3-1). No ABR waveforms were determined in any aged DBA mice even by stimuli at 100 dB SPL; the ABR thresholds for these animals were determined to be 100.0 dB SPL at all frequency tested, indicating severe hearing loss (Figure 3-1). These results show that aged DBA mice exhibit age-related profound hearing loss.

Histology

Histological analysis revealed that aged DBA mice exhibited severe loss of outer hair cells, inner hair cells, and supporting cells in the organ of Corti, and severe loss of spiral ganglion cells in the cochlea, whereas control DBA mice exhibited mild degeneration of the organ of Corti (Figure 3-2). These results support the ABR findings,

Gene Expression Analysis

To examine transcriptional changes induced by AHL, I used oligonucleotide arrays representing 22,626 genes and ESTs. A comparison of the cochlea from the control DBA mice and the aged DBA mice revealed that AHL is associated with significant alterations in mRNA levels. Of the 22,626 genes and ESTs surveyed in the oligonucleotide arrays, we identified 99

Figure 3-1. Comparison of ABR thresholds. ABR thresholds were measured at 4 kHz, 8 kHz, and 16 kHz. The 7-week-old DBA mice (control, n = 5) exhibited moderate hearing loss, whereas the 36-week-old DBA mice (aged, n = 5) exhibited severe hearing loss.

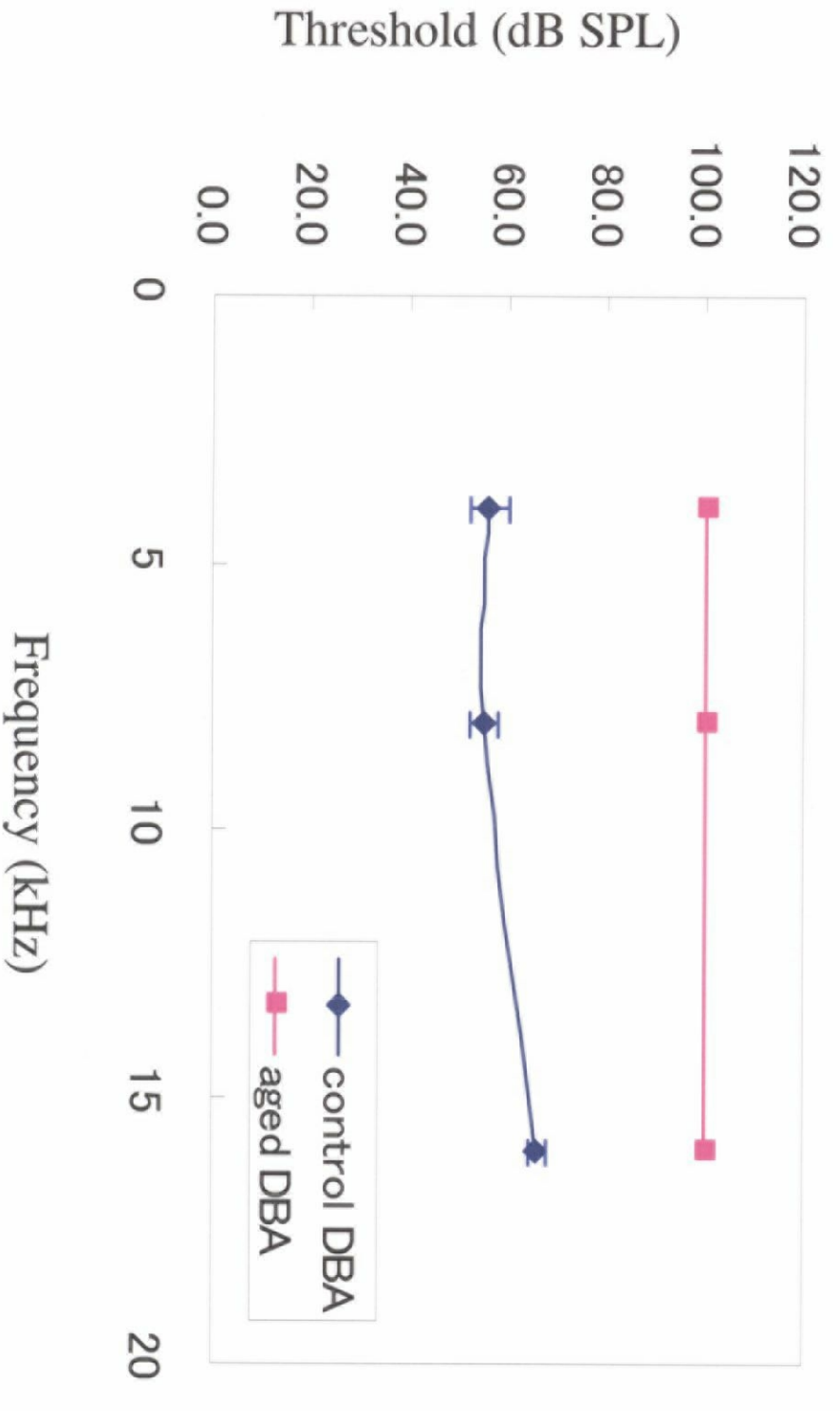
Threshold (dB SPL)
120.0
100.0
80.0
60.0
40.0
20.0
0.0
0
5
10
15
20
Frequency (kHz)
control DBA
aged DBA

Figure 3-2. Comparison of cochleae. Representative light micrographs of the lower basal cochlear turn from the 7-week-old DBA mouse (control) and the 36-week-old DBA mouse (aged). The aged DBA mouse exhibited severe loss of outer hair cells (OHC), inner hair cells (IHC), and supporting cell in the organ of Corti, and severe loss of spiral ganglion cells (SGC) in the cochlea, whereas the control DBA mouse showed mild degeneration of the organ of Corti in the cochlea.

control DBA

aged DBA

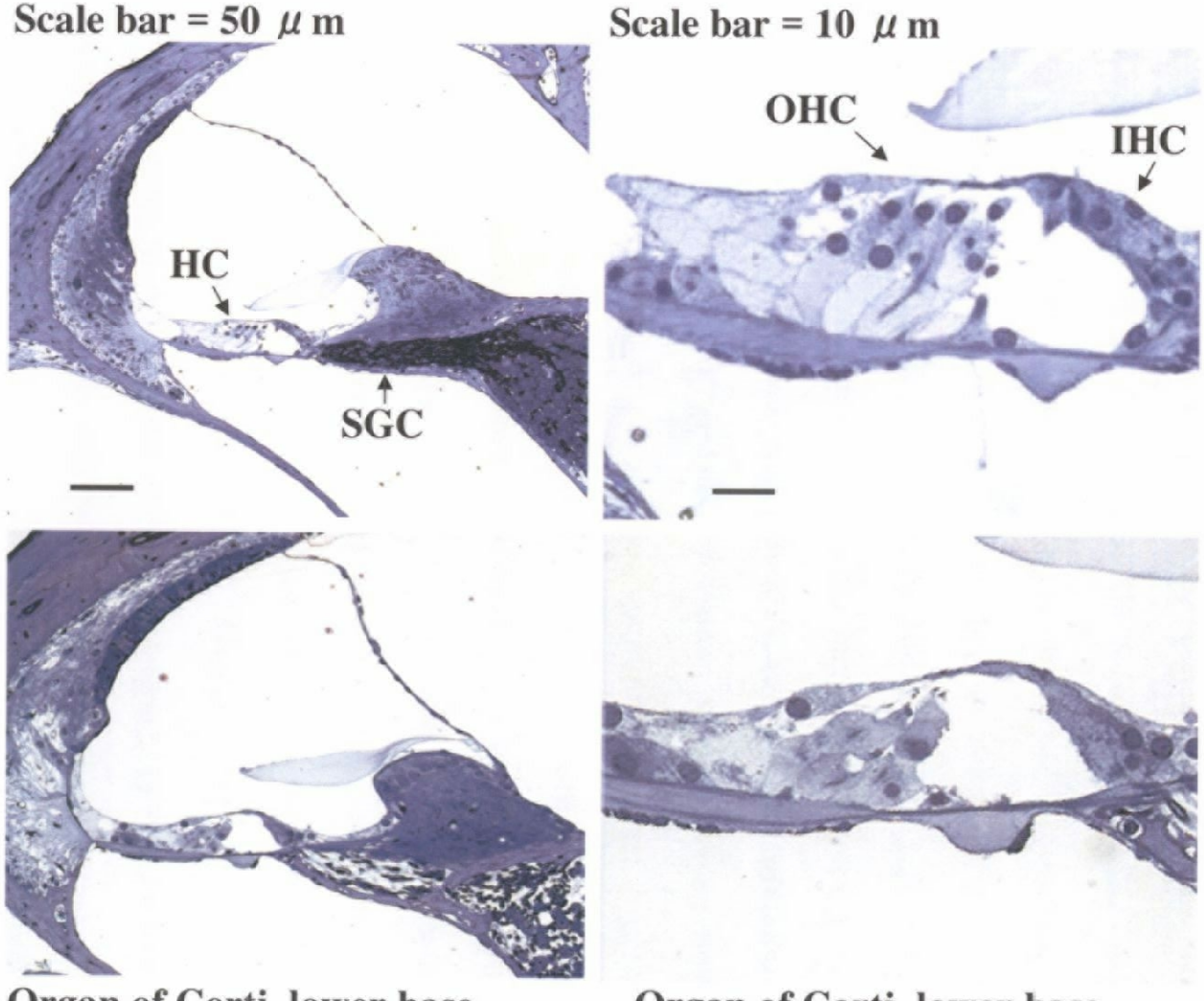

Organ of Corti, lower base

Organ of Corti, lower base

genes down-regulated by AHL and 57 genes up-regulated by AHL (Table 3-1). Of the 99 genes that decreased with AHL, 17 genes were hearing-related genes, such as potassium voltage-gated channel, Isk-related subfamily, member 1 (*Kcne1*), otospiralin (*Otos*), solute carrier family 26, member 4 (*Slc26a4*), insulin-like growth factor 1 (*Igf1*), gap junction membrane channel protein beta 6 (*Gjb6*), and coagulation factor C homolog (*limulus polyphemus*) (*Coch*). These results were consistent with those of the ABR analysis and the histology analysis. The gene with the largest downregulation in this transcriptional class was Kcne1 gene (fold change = -12.0). This gene is expressed in the inner hair cells, and Kcne1 protein mediates potassium secretion into the endolymph (Vetter *et al.*, 1996). Mutations in the gene are considered to cause a non-syndromic, progressive hearing loss (Vetter *et al.*, 1996). Otos gene is expressed in glical cells surrounding the spiral ganglion cells in the cochlea, and Otos protein is essential for survival of neurosensory epithelium (Delprat *et al.*, 2002). Downregulation of this gene is thought to causes hair cells degeneration and deafness (Delprat *et al.*, 2002). Gjb6 gene is expressed in supporting cells in the organ of Corti. Gjb6 protein is a member of connexins involved in formation of gap junctions between cells (Forge *et al.*, 2003; Kelley *et al.*, 1999). Mutations in this gene are thought to cause non-syndromic autosomal recessive deafness (Forge *et al.*, 2003; Kelley *et al.*, 1999). Seven genes involved in energy metabolism, such as cytochrome c oxidase, subunit VIIa1 (*Cox7a1*), lactate dehydrogenasae 2, B chanin (*Ldh2*), ATP synthase, H^+ transporting, mitochondrial F0 complex, subunit F (*Atp5j*), NADH

Table 3-1. List of selected genes altered in the expression by AHL. This table lists genes of selected classes that were significantly (*P* value = 0.01 >, FC = 1.2 ≦) altered in the gene expression with AHL. 22,626 genes and ESTs were screened using GeneChips (MOE 430A). The fold change shown represents the average of all nine possible pairwise comparisons among individual samples (n = 3 for each group) determined by the Microarray Suit Expression Analysis software. GenBank accession numbers are listed under Gene ID.

Gene ID	FC	Gene
Perception of Sound		
NM_008424	-12.0	potassium voltage-gated channel, Isk-related subfamily, member 1
AY078071	-6.0	otospiralin
NM_011867	-5.1	solute carrier family 26, member 4
BG075165	-4.0	insulin-like growth factor 1
BC016507	-4.0	gap junction membrane channel protein beta 6
BB731671	-3.6	coagulation factor C homolog (Limulus polyphemus)
AV239646	-3.6	gap junction membrane channel protein beta 2
BB763517	-3.5	microphthalmia-associated transcription factor
NM_011390	-2.8	solute carrier family 12, member 7
BB836814	-2.7	procollagen, type XI, alpha 1
X66603	-2.6	POU domain, class 3, transcription factor 4
AY055122	-2.4	otoancorin
U13174	-2.4	solute carrier family 12, member 2
AV242706	-2.2	procollagen, type XI, alpha 2
NM_008885	-1.9	peripheral myelin protein
BB732903	-1.8	fibroblast growth factor receptor 3
NM_009866	-1.6	cadherin 11
Energy Metabolism		
AF037370	-3.1	cytochrome c oxidase, subunit VIIa 1
AV219418	-1.9	lactate dehydrogenase 2, B chain

(*continued*)

Gene ID	FC	Gene
NM_016755	-1.7	ATP synthase, H+ transporting, mitochondrial F0 complex, subunit F
NM_026614	-1.6	NADH dehydrogenase (ubiquinone) 1 alpha subcomplex, 5
W29413	-1.6	NADH dehydrogenase (ubiquinone) 1 beta subcomplex, 9
AV216686	-1.5	ATP synthase, H+ transporting, mitochondrial F1F0 complex, subunit e
BI692577	-1.5	NADH dehydrogenase (ubiquinone) flavoprotein 2
Neurotransmission/Neuronal Factors		
NM_009115	-3.4	S100 protein, beta polypeptide, neural
D10727	-2.7	enabled homolog (Drosophila)
BB768495	-1.9	proteolipid protein (myelin)
BC014803	-1.6	complexin 1
BC018383	-1.6	internexin neuronal intermediate filament protein, alpha
BQ175915	-1.6	ATPase, Na+/K+ transporting, alpha 2 polypeptide
Apoptosis		
NM_009402	17.8	peptidoglycan recognition protein 1
NM_019391	3.4	lymphocyte specific 1
NM_007523	2.4	BCL2-antagonist/killer 1
BB151515	2.1	nerve growth factor receptor (TNFR superfamily, member 16)
BG075396	2.0	transcription factor Dp 1
BG084230	1.9	PYD and CARD domain containing
NM_007467	1.7	amyloid beta (A4) precursor-like protein 1
AI323543	1.7	phosphoprotein enriched in astrocytes 15

(*continued*)

Gene ID	FC	Gene
BC010238	1.7	scotin gene
AV173139	1.5	serine/threonine kinase 17b (apoptosis-inducing)
BF384094	1.5	eukaryotic translation initiation factor 5A
AJ005074	1.5	programmed cell death 6 interacting protein
BC003839	1.4	myeloid cell leukemia sequence 1
BI219063	1.4	glutathione peroxidase 1
BC005588	1.4	testis enhanced gene transcript
AF100339	1.4	B-cell leukemia/lymphoma 10
BC027307	1.3	BCL2-like 13 (apoptosis facilitator)
NM_007377	1.2	apoptosis-associated tyrosine kinase
Stress Response		
NM_010824	12.1	myeloperoxidase
AF059486	5.6	advillin
BE632222	3.1	protein phosphatase 3, catalytic subunit, alpha isoform
NM_007946	2.8	eosinophil peroxidase
AF401228	2.1	neuralized homolog (Drosophila)
NM_026322	1.7	methionine sulfoxide reductase A
Inflammatory Response/Immune Modulation		
AF466769	75.8	immunoglobulin heavy chain 4 (serum IgG1)
NM_011260	39.1	regenerating islet-derived 3 gamma
NM_009921	23.5	cathelicidin antimicrobial peptide

(*continued*)

Gene ID	FC	Gene
U72644	16.0	leukocyte specific transcript 1
NM_011093	14.6	paired-Ig-like receptor B
K02782	14.1	complement component 3
NM_008694	14.1	neutrophilic granule protein
NM_009892	11.8	chitinase 3-like 3
AV058500	8.1	P lysozyme structural
BC002073	7.6	chemokine (C-C motif) ligand 6
BC026209	7.6	arachidonate 5-lipoxygenase activating protein
AK008145	7.3	immunoglobulin lambda chain, variable 1
AW208566	6.5	lysozyme
NM_017388	6.1	eosinophil-associated, ribonuclease A family, member 2
M36005	3.7	selectin, lymphocyte
D87747	3.2	chemokine (C-X-C motif) receptor 4
M86502	3.0	histocompatibility 2, K1, K region
NM_010741	2.9	lymphocyte antigen 6 complex, locus C
NM_010188	2.8	Fc receptor, IgG, low affinity III
M33151	2.3	histocompatibility 2, Q region locus 10
D87968	2.2	protein tyrosine phosphatase, non-receptor type substrate 1
AF251036	2.0	protein kinase C, delta
AK010883	1.9	Duffy blood group
BC003476	1.7	Ia-associated invariant chain

(*continued*)

Gene ID	FC	Gene
X00246	1.6	histocompatibility 2, D region locus 1
BC005409	1.6	thyroid hormone receptor associated protein 4
Proteolysis and peptidolysis/Catabolism		
NM_017370	52.8	haptoglobin
AF369933	20.3	mucin 5, subtype B, tracheobronchial
U97073	20.0	proteinase 3
NM_007800	18.1	cathepsin G
NM_008611	17.3	matrix metalloproteinase 8
NM_013599	13.7	matrix metalloproteinase 9
NM_009982	2.3	cathepsin C
Ion Transport		
NM_008424	-12.0	potassium voltage-gated channel, Isk-related subfamily, member 1
BB497312	-4.0	solute carrier family 13 (sodium-dependent dicarboxylate transporter), member 3
AF440692	-3.4	transferrin
BB667135	-2.7	solute carrier organic anion transporter family, member 1c1
BB332449	-2.4	ceruloplasmin
U13174	-2.4	solute carrier family 12, member 2
BI080505	-2.2	ATPase, Na+/K+ transporting, beta 3 polypeptide
AV152334	-1.9	ATPase, Na+/K+ transporting, beta 1 polypeptide
BC024613	-1.8	protein distantly related to to the gamma subunit family
AF014010	-1.8	polycystic kidney disease 2

(*continued*)

Gene ID	FC	Gene
NM_010239	-1.5	ferritin heavy chain
Muscle Contraction/Muscle Modulation		
X67685	-45.3	myosin, light polypeptide 3
NM_022314	-6.9	tropomyosin 3, gamma
M12233	-4.2	actin, alpha 1, skeletal muscle
BI248947	-3.4	caldesmon 1
NM_009393	-3.3	troponin C, cardiac/slow skeletal
NM_009394	-3.1	troponin C2, fast
NM_009405	-3.1	troponin I, skeletal, fast 2
NM_011620	-2.9	troponin T3, skeletal, fast
NM_033268	-2.8	actinin alpha 2
AK002271	-2.7	tropomyosin 1, alpha
NM_025357	-2.6	small muscle protein, X-linked
AJ002522	-2.4	myosin, heavy polypeptide 1, skeletal muscle, adult
AJ278733	-2.4	myosin, heavy polypeptide 4, skeletal muscle
NM_007504	-2.1	ATPase, Ca++ transporting, cardiac muscle, fast twitch 1
BB833102	-2.0	calponin 3, acidic
AK007972	-1.9	myosin, light polypeptide 9, regulatory
NM_009416	-1.7	tropomyosin 2, beta
Structure/Structural Modulation		
AA223007	-5.4	nephronectin

(*continued*)

Gene ID	FC	Gene
NM_016754	-4.9	myosin light chain, phosphorylatable, fast skeletal muscle
NM_010861	-3.9	myosin, light polypeptide 2, regulatory, cardiac, slow
AK010167	-3.7	titin-cap
BC025840	-3.5	titin
NM_008770	-3.3	claudin 11
NM_009263	-2.7	secreted phosphoprotein 1
BG968894	-2.7	procollagen, type III, alpha 1
NM_008597	-2.3	matrix gamma-carboxyglutamate (gla) protein
AI642438	-2.2	lectin, galactose binding, soluble 1
AV242706	-2.2	procollagen, type XI, alpha 2
AV230775	-2.0	keratin complex 2, basic, gene 17
BE994235	-1.9	pleckstrin homology domain containing, family C (with FERM domain) member 1
AK019164	-1.9	multiple PDZ domain protein
NM_008473	-1.7	keratin complex 2, basic, gene 1
NM_009866	-1.6	cadherin 11
BG075070	-1.6	erythrocyte protein band 4.1-like 2
BF227507	-1.6	procollagen, type I, alpha 2
Growth Factors/Development		
BG075165	-4.0	insulin-like growth factor 1
NM_007556	-2.7	bone morphogenetic protein 6
AK011784	-2.6	insulin-like growth factor binding protein 2

(*continued*)

Gene ID	FC	Gene
BB542051	-2.5	osteoglycin
NM_008344	-2.4	insulin-like growth factor binding protein 6
BF225802	-2.4	insulin-like growth factor binding protein 5
AK004853	-2.0	dickkopf homolog 3 (Xenopus laevis)
AU018448	-1.9	pituitary tumor-transforming 1 interacting protein
BG085921	-1.9	cyclin G1
BQ175880	-1.9	cyclin D2
NM_026162	-1.6	plexin domain containing 2
Biosynthesis		
NM_010024	-4.2	dopachrome tautomerase
AB006361	-3.5	prostaglandin D2 synthase (brain)
BG141874	-3.5	transthyretin
NM_008968	-2.7	prostaglandin I2 (prostacyclin) synthase
BC016885	-2.5	UDP-glucuronosyltransferase 8
C81193	-2.3	ornithine decarboxylase, structural
NM_015786	-2.1	histone 1, H1c
DNA Synthesis/DNA Repair		
AW049660	-1.9	nuclear factor I/X
NM_008251	-1.7	high mobility group nucleosomal binding domain 1
Protein Synthesis/Modification		
NM_008812	-2.0	peptidyl arginine deiminase, type II

(*continued*)

Gene ID	FC	Gene
AK002778	-1.5	eukaryotic translation initiation factor 3, subunit 5 (epsilon)
Fatty Acid Metabolism		
AF277093	-1.8	elongation of very long chain fatty acids (FEN1/Elo2, SUR4/Elo3, yeast)-like 4

dehydrogenase (ubiquinone) 1 alpha subcomplex, 5 (Ndufa5), and ATP synthase, H^+ transporting, mitochondrial F1F0 complex, subunit e (*Atp5k*), also displayed a decrease in the gene expression. These results correlate well with the studies of mitochondria mutations and hearing loss, which suggest that mitochondrial dysfunction may be associated with AHL (Damdimpopoulos *et al.*, 2002; Fischel-Ghodsian, 1999; Johnson *et al.*, 2001; Seidman *et al.*, 2002). The gene with the largest downregulation in this transcriptional class was Cox7a1 gene (fold change = -3.1). This gene is expressed in mitochondria in numerous tissues, and Cox7a1 protein is involved in cytochrome c oxidase activity (Mootha *et al.*, 2003). Atp5j protein is involved in hydrogen-transporting ATP synthase activity in mitochondria (Mootha *et al.*, 2003), and Ndufa5 protein is involved in NADH dehydrogenase (ubiquinone) activity in mitochondria (Mootha *et al.*, 2003). AHL also lowered the gene expression of six neurotransmission-related genes, including S100 protein, beta polypeptide, neural (*S100b*), enabled homolog (*Drosophila*) (*Enah*), and proteolipid protein (myelin) (*Plp*). The gene with the largest downregulation in this transcriptional class was S100b gene (fold change = -3.4). The S100 protein family is the largest subgroup within the superfamily of proteins carrying the Ca2+-binding EF-hand motif. Various diseases such as cardiomyopathies, neurodegenerative and inflammatory disorders, and cancer are associated with altered S100 protein levels (Marenholz *et al.*, 2004).

AHL induced 18 apoptosis-related genes, such as peptidoglycan

recognition protein 1 (*Pglyrp1*), BCL2-antagonist/Killer 1 (*Bak1*), PYD and CARD domain containing (*Pycard*), Scotin gene (*Scotin*), and eukaryotic translation initiation factor 5A (*Eif5a*). These results were consistent with the histological findings. These results also correlate well with the studies of apoptosis and AHL, which show that apoptosis may be associated with AHL (Fischel-Ghodsian, 1999; Seidman, 2002; Dirks and Leeuwenburgh, 2002). The gene with the largest upregulation in this transcriptional class was *Pglyrp1* (fold change = 17.8). The Pglyrp1 protein induces apoptotic death in several tumor-derived cell lines by interacting with the Hsp70 (Sashchenko *et al.*, 2003). p53 is a transcription factor that induces growth arrest or apoptosis in response to cellular stress, and it has a direct signaling role at mitochondria in induction of apoptosis (Prives and Hall, 1999; Vogelstein *et al.*, 2000). p53 activates Bak1 gene, which causes release of cytochrome c from mitochondria, and hence to induction of apoptosis (Berlin, 2000; Johnson *et al.*, 1997; Jimenez *et al.*, 2001; Keithley *et al.*, 2003). p53 also activates Scotin gene, which in turn induce apoptosis (Bourdon *et al.*, 2002). Six genes involved in stress response, such as myeloperoxidase (*Mpo*), advillin (*Avil*), protein phosphatase 3, catalytic subunit, alpha isoform (*Ppp3ca*), eosinophil peroxidase (Epx), and methionine sulfoxide reductase A (Msra), also displayed an increase in the gene expression. These results correlate well with the studies of oxidative stress in AHL, which suggest that oxidative stress, which is caused by mitochondrial dysfunction, may be associated with AHL (Staecker *et al.*, 2001; Coling *et al.*, 2003). The gene with the largest upregulation in this transcriptional class was *Mpo* (fold

change = 12.1). Mpo protein is involved in response to oxidative stress, and catalyzes the reaction of hydrogen peroxide with chloride ion to produce hypochlorous acid (Aratani *et al.*, 1999). AHL induced the gene expression of 26 inflammatory response-related genes, including immunoglobulin heavy chain 4 (serum IgG1), regenerating islet-derived 3 gamma, cathelicidin antimicrobial peptide, Leukocyte specific transcript 1, and paired-Ig-like receptor B. These results were consistent with the histological findings since severe degeneration of cells was found in the AHL cochlea. AHL also induced the gene expression of 7 proteolysis-related genes including haptoglobin, mucin 5, subtype B, tracheobronchial, and proteinase 3.

AHL lowered the gene expression of 11 ion transport-related genes including, potassium voltage-gated channel, Isk-related subfamily, member 1, solute carrier family 13 (sodium-dependent dicarboxylate transporter), member 3, and transferring. AHL also lowered transcripts associated with muscle contraction, such as myosin, light polypeptide 3, tropomyosin 3, gamma, and actin, alpha 1, skeletal muscle. AHL was also characterized by reductions in the gene expression for genes involved in structural modulation, growth factor, biosynthesis, DNA synthesis, DNA repair, protein synthesis, and fatty acid metabolism.

Summary of findings

A summary of global view of transcriptional changes induced by AHL is shown in Table 3-2. These results revealed that AHL results in

Table 3-2. Global view of transcriptional changes induced by AHL. This table lists selected classes of transcriptional changes induced by AHL.

Function	FC	Description
Perception of Sound	↓	Suppression of hearing-related genes
Energy metabolism	↓	Mitochondrial dysfunction, Reduced glycolysis
Neurotransmission/Neuronal Factors	↓	Decreased neurotransmitter transport, neurogenesis
Apoptosis	↑	Induction of apoptosis
Stress Response	↑	Induction of oxidative stress-inducible genes
Inflammatory Response	↑	Induction of inflammatory response, immune response
Proteolysis and Peptidolysis	↑	Increased proteolysis and peptidolysis
Ion Transport	↓	Decreased potassium ion transport, sodium ion transport,
Muscle Contraction/Muscle Modulation	↓	Suppression of muscle contraction and muscle development
Structure/Structural Modulation	↓	Suppression of cytoskeleton organization and cell adhesion
Growth Factors/Development	↓	Suppression of cell growth and cell differentiation
Biosynthesis	↓	Decreased glycolipid biosynthesis and prostaglandin biosynthesis
DNA Synthesis/DNA Repair	↓	Suppression of DNA replication factors and DNA repair factors
Protein Synthesis/Modification	↓	Decreased protein biosynthesis and protein modification
Fatty Acid Metabolism	↓	Reduced fatty acid biosynthesis

suppression of hearing-related genes, decreased energy metabolism, and induction of apoptosis-related genes, such as *Bak1* and *Scotin*, which mediate p53-dpendent apoptosis (Leu *et al.*, 2004; Degenhardt *et al.*, 2002; Bourdon *et al.*, 2002), and increased stress response. AHL was also characterized by reductions in the gene expression for genes involved in ion transport, muscle contraction, structural modulation, growth factor, biosynthesis, DNA synthesis, DNA repair, protein synthesis, and fatty acid metabolism. Mitochondrial dysfunction may induce apoptosis, which in turn leads to loss of vulnerable cells in the cochlea (Fischel-Ghodsian, 1999). Thus, these results suggest that AHL develops by mechanisms that may be related to mitochondrial dysfunction and induction of apoptosis.